

## TABLE OF CONTENTS

	<b>Page</b>
Acknowledgement	iii
Abstract (in English)	v
Abstract (in Thai)	vii
List of tables	xiii
List of figures	xvii
Abbreviations and symbols	xxx
<b>CHAPTER 1 INTRODUCTION</b>	<b>1</b>
1.1 Definition and classification of inorganic–organic hybrid materials	3
1.2 Synthesis and single crystal growth of inorganic–organic hybrid compounds	6
1.3 Overview on first–row transition metal–organic hybrid materials	7
1.4 Recent overview on the lanthanide metal–organic hybrid materials	11
1.5 Research objectives	14
1.6 Research plan	15
<b>CHAPTER 2 PREPARATION AND CHARACTERIZATION OF BIS(1,2–DIAMINOETHANE) COBALT(II) HEXAVANADATE: A LAYERED POLYOXOVANADATE PILLARED BY A COBALT COORDINATION COMPLEX</b>	<b>20</b>
<b>2.1 Experimental</b>	<b>21</b>

2.1.1 Synthesis and initial characterization	21
2.1.2 Single crystal structure determination	22
<b>2.2 Results and discussion</b>	<b>22</b>
2.2.1 Structural description	22
2.2.2 FT – IR spectra of compound <b>I</b>	31
<b>2.3 Conclusions</b>	<b>32</b>
<b>CHAPTER 3 MICROWAVE SYNTHESIS AND CRYSTAL</b>	<b>35</b>
<b>STRUCTURES OF TWO COBALT–4,4'–BIPYRIDINE–SULFATE</b>	
<b>FRAMEWORKS CONSTRUCTED FROM 1–D COORDINATION</b>	
<b>POLYMERS LINKED BY HYDROGEN BONDING</b>	
<b>3.1 Materials and methods</b>	<b>37</b>
3.1.1 Microwave–assisted hydrothermal crystal growth	37
3.1.2 X–ray diffraction structure determination	38
3.1.3 Spectroscopic studies of <b>III</b> and <b>IV</b>	39
<b>3.2 Results and discussion</b>	<b>39</b>
3.2.1 Microwave synthesis	39
3.2.2 Bipyridinium–templated phase, <b>III</b>	40
3.2.3 Sulfate–decorated coordination polymer, <b>IV</b>	51
3.2.4 Thermogravimetric studies of compound <b>III</b> and <b>IV</b>	62
3.2.5 Spectroscopic characterization of <b>III</b> and <b>IV</b>	64
3.2.5.1 Vibrational spectra of <b>III</b> and <b>IV</b>	64
3.2.5.2 UV–Vis spectra of <b>III</b> and <b>IV</b>	67
<b>3.3 Conclusions</b>	<b>68</b>

**CHAPTER 4 LANTHANIDE SULFATE –4,4'–BIPYRIDINE 71**

**FRAMEWORKS: SYNTHESIS, STRUCTURE, AND OPTICAL PROPERTIES**

**4.1 Experimental section 72**

4.1.1 Synthesis and initial characterization 72

4.1.2 Single crystal structure determination 77

4.1.3 Photoluminescence measurements of  $\text{Eu}^{\text{III}}/\text{Tb}^{\text{III}}$ -doped compounds 79

**4.2 Results and discussion 79**

4.2.1 Structure of  $[\text{C}_{10}\text{H}_{10}\text{N}_2]_{0.5}[\text{La}(\text{SO}_4)_2]\cdot\text{H}_2\text{O}$  (V) 79

4.2.2 Structure of  $[\text{C}_{10}\text{H}_{10}\text{N}_2]_{0.5}[\text{Pr}(\text{SO}_4)_2(\text{H}_2\text{O})_2]$  (VIb) 84

4.2.3 Structure of  $[\text{C}_{10}\text{H}_{10}\text{N}_2][\text{Ln}_2(\text{SO}_4)_4(\text{H}_2\text{O})_2]$ ,  $\text{Ln} = \text{Nd}^{\text{III}}$  (VIIa),  $\text{Sm}^{\text{III}}$  (VIIb), and  $\text{Eu}^{\text{III}}$  (VIIc) 90

4.2.4 Structural comparison 96

4.2.5 Thermogravimetric studies 98

4.2.6 Luminescence studies 100

4.2.7 Lifetime studies 101

4.2.8 Upconversion studies 105

**4.3 Conclusions 110**

**CHAPTER 5 SYNTHESIS, STRUCTURE AND PHOTO– 113**

**LUMINESCENCE PROPERTY OF NEW 1-D LANTHANUM SULFATE–*o*– PHENANTHROLINE COORDINATION POLYMER**

<b>5.1 Experimental</b>	114
5.1.1 Synthesis and characterization	114
5.1.2 Determination of the crystal structure	115
5.1.3 Photoluminescence measurements of Eu <sup>III</sup> /Tb <sup>III</sup> -doped compounds	118
<b>5.2 Results and discussion</b>	118
5.2.1 Description of the crystal structure	118
5.2.2 IR and UV-Vis spectroscopic studies	129
5.2.3 Thermogravimetric analysis	131
5.2.4 Photoluminescence studies of the Eu <sup>III</sup> /Tb <sup>III</sup> doped- [La <sub>2</sub> ( <i>o-phen</i> ) <sub>2</sub> (SO <sub>4</sub> ) <sub>3</sub> (H <sub>2</sub> O) <sub>2</sub> ] <sub>n</sub>	134
<b>5.3 Conclusions</b>	136
<b>CHAPTER 6 SYNTHESIS AND CRYSTAL STRUCTURES OF NEW LANTHANIDE FRAMEWORKS WITH A FLEXIBLE POLYCARBOXYLATE LIGAND</b>	<b>139</b>
<b>6.1 Experimental</b>	141
6.1.1 Synthesis and crystal growth	141
6.1.2 Single Crystal Structure Determination	143
<b>6.2 Results and discussion</b>	152
6.2.1 Crystal structures of [Ln <sub>4</sub> (C <sub>15</sub> H <sub>12</sub> O <sub>12</sub> N <sub>6</sub> ) <sub>2</sub> (C <sub>8</sub> H <sub>10</sub> N <sub>2</sub> O <sub>6</sub> ) <sub>0.5</sub> (H <sub>2</sub> O) <sub>3</sub> ].5H <sub>2</sub> O, Ln = Pr <sup>III</sup> ( <b>IXa</b> ) and Nd <sup>III</sup> ( <b>IXb</b> )	154
6.2.2 Crystal structure of [Sm <sub>8</sub> (C <sub>15</sub> H <sub>12</sub> O <sub>12</sub> N <sub>6</sub> ) <sub>4</sub> (C <sub>8</sub> H <sub>10</sub> N <sub>2</sub> O <sub>6</sub> ) <sub>0.5</sub> (H <sub>2</sub> O) <sub>8</sub> ].4H <sub>2</sub> O ( <b>X</b> )	163

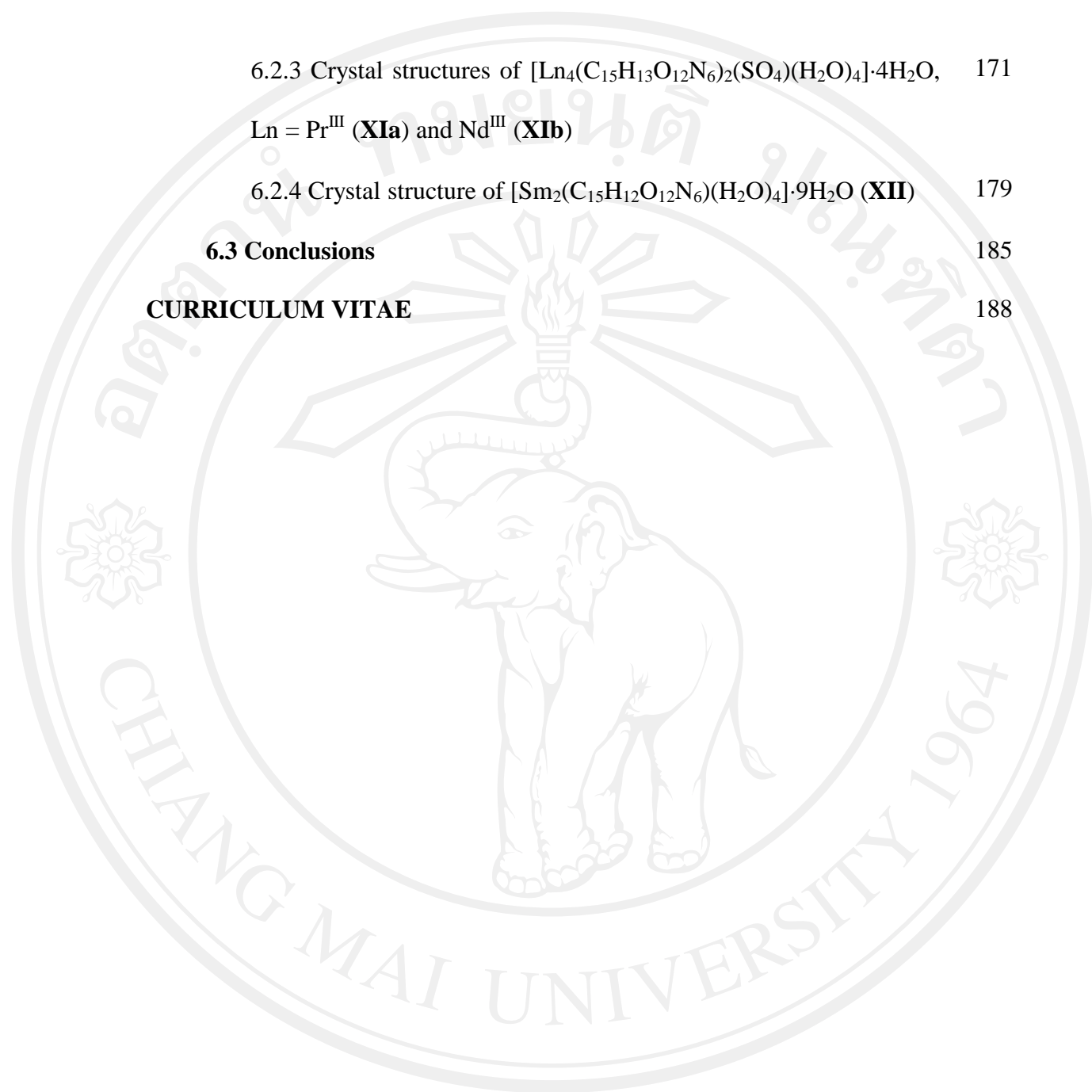
6.2.3 Crystal structures of  $[\text{Ln}_4(\text{C}_{15}\text{H}_{13}\text{O}_{12}\text{N}_6)_2(\text{SO}_4)(\text{H}_2\text{O})_4]\cdot 4\text{H}_2\text{O}$ , 171

$\text{Ln} = \text{Pr}^{\text{III}}$  (**XIa**) and  $\text{Nd}^{\text{III}}$  (**XIb**)

6.2.4 Crystal structure of  $[\text{Sm}_2(\text{C}_{15}\text{H}_{12}\text{O}_{12}\text{N}_6)(\text{H}_2\text{O})_4]\cdot 9\text{H}_2\text{O}$  (**XII**) 179

**6.3 Conclusions** 185

**CURRICULUM VITAE** 188



ลิขสิทธิ์มหาวิทยาลัยเชียงใหม่

Copyright© by Chiang Mai University  
All rights reserved

## LIST OF TABLES

<b>Table</b>		<b>Page</b>
2.1	Crystallographic data for structural solution and refinement of <b>I</b> .	23
2.2	Atomic coordinates ( $\times 10^4$ ) and equivalent isotropic displacement parameters ( $\text{\AA}^2 \times 10^3$ ) of non-hydrogen atoms for <b>I</b> .	24
2.3	Selected bond distances and angles for compound <b>I</b> .	26
2.4	Hydrogen bonding geometry for <b>I</b> .	29
3.1	Summary of crystal and refinement data for <b>III</b> and <b>IV</b> .	41
3.2	Atomic coordinates ( $\times 10^4$ ) and equivalent isotropic displacement parameters ( $\text{\AA}^2 \times 10^3$ ) for <b>III</b> .	42
3.3	Selected observed bond distances and angles in the compound <b>III</b> .	45
3.4	Details of the classical hydrogen bonds and C–H...O interactions in <b>III</b> . A hydrogen bond donor is signified as D–H, where D is the donor atom. The hydrogen bond acceptor atom is labeled A.	47
3.5	Atomic coordinates ( $\times 10^4$ ) and equivalent isotropic displacement parameters ( $\text{\AA}^2 \times 10^3$ ) for <b>IV</b> .	53
3.6	Selected observed bond distances in the compound <b>IV</b> .	56

3.7	Details of the classical hydrogen bonds and C–H...O interactions in	61
	<b>IV.</b> A hydrogen bond donor is signified as D–H, where D is the donor atom. The hydrogen bond acceptor atom is labeled A.	
4.1	Synthesis conditions employed for the compounds.	73
4.2	Crystal data and structure refinement parameters for the compounds [C <sub>10</sub> H <sub>10</sub> N <sub>2</sub> ] <sub>0.5</sub> [La(SO <sub>4</sub> ) <sub>2</sub> ].H <sub>2</sub> O, ( <b>V</b> ) [C <sub>10</sub> H <sub>10</sub> N <sub>2</sub> ] <sub>0.5</sub> [Pr(SO <sub>4</sub> ) <sub>2</sub> (H <sub>2</sub> O) <sub>2</sub> ], ( <b>VIb</b> ), and [C <sub>10</sub> H <sub>10</sub> N <sub>2</sub> ][Ln <sub>2</sub> (SO <sub>4</sub> ) <sub>4</sub> (H <sub>2</sub> O) <sub>2</sub> ] <sub>2</sub> , (Ln= Nd ( <b>VIIa</b> ), Sm ( <b>VIIb</b> ) and Eu ( <b>VIIc</b> ).	78
4.3	Selected observed bond distances in the compound <b>V</b> .	82
4.4	Atomic coordinates ( $\times 10^4$ ) and equivalent isotropic displacement parameters ( $\text{\AA}^2 \times 10^3$ ) for <b>V</b> .	82
4.5	Details of the hydrogen bonds interactions in <b>V</b> . A hydrogen bond donor is signified as D–H, where D is the donor atom. The hydrogen bond acceptor atom is labeled A.	84
4.6	Selected observed bond distances in the compound <b>VIb</b> .	86
4.7	Atomic coordinates ( $\times 10^4$ ) and equivalent isotropic displacement parameters ( $\text{\AA}^2 \times 10^3$ ) for <b>VIb</b> .	86
4.8	Details of the hydrogen bonds interactions in <b>VIb</b> . A hydrogen bond donor is signified as D–H, where D is the donor atom. The hydrogen bond acceptor atom is labeled A.	87
4.9	Selected observed bond distances and angles in the compound <b>VIIa</b> .	92
4.10	Atomic coordinates ( $\times 10^4$ ) and equivalent isotropic displacement parameters ( $\text{\AA}^2 \times 10^3$ ) for <b>VIIa</b> .	92

4.11	Details of the hydrogen bonds interactions in <b>VIIa</b> . A hydrogen bond donor is signified as D–H, where D is the donor atom. The hydrogen bond acceptor atom is labeled A.	96
4.12	Lifetime values for the compounds <b>V</b> (4% Eu), <b>VIa</b> (4% Eu), <b>V</b> (4% Tb), and <b>VIa</b> (4% Tb).	104
5.1	Crystallographic data for structural solution and refinement of <b>VIII</b> .	116
5.2	Selected bond lengths (Å) and angles of compound <b>VIII</b> .	117
5.3	Details of the hydrogen bonds interactions in <b>VIII</b> . A hydrogen bond donor is signified as D–H, where D is the donor atom. The hydrogen bond acceptor atom is labeled A.	124
5.4	List of assignments for the IR spectra of the pristine $[\text{La}_2(o\text{-phen})_2(\text{SO}_4)_3(\text{H}_2\text{O})_2]_n$ and the brown powder obtained after the treatment at 600°C.	130
6.1	Synthetic conditions employed for the synthesis of <b>IXa</b> , <b>IXb</b> , <b>X</b> , <b>XIa</b> , <b>XIb</b> and <b>XII</b> .	142
6.2	Crystal data and structure refinement parameters for <b>IXa</b> , <b>IXb</b> , <b>X</b> , <b>XIa</b> , <b>XIb</b> and <b>XII</b> .	144
6.3	Atomic coordinates ( $\times 10^4$ ) and equivalent isotropic displacement parameters ( $\text{\AA}^2 \times 10^3$ ) for <b>IXa</b> .	145
6.4	Atomic coordinates ( $\times 10^4$ ) and equivalent isotropic displacement parameters ( $\text{\AA}^2 \times 10^3$ ) for <b>X</b> .	146
6.5	Atomic coordinates ( $\times 10^4$ ) and equivalent isotropic displacement parameters ( $\text{\AA}^2 \times 10^3$ ) for <b>XIa</b> .	149

6.6	Atomic coordinates ( $\times 10^4$ ) and equivalent isotropic displacement parameters ( $\text{\AA}^2 \times 10^3$ ) for <b>XII</b> .	150
6.7	Selected bond distances in the compound <b>IXa</b> .	151
6.8	Selected bond distances in the compound <b>X</b> .	151
6.9	Selected bond distances in the compound <b>XIa</b> .	152
6.10	Selected bond distances in the compound <b>XII</b> .	152
6.11	Coordination modes of the carboxylates in TTHA and <i>L2</i> ligands.	158
6.12	List of hydrogen bonding interactions and geometries in <b>IXa</b> .	162
6.13	List of the hydrogen bonding interactions in <b>X</b> .	171
6.14	List of the hydrogen bonding interactions and geometries in <b>XIa</b> .	179
6.15	List of the hydrogen bonding interactions and geometries in <b>XII</b> .	184

ลิขสิทธิ์มหาวิทยาลัยเชียงใหม่

Copyright© by Chiang Mai University  
All rights reserved

## LIST OF FIGURES

<b>Figure</b>		<b>Page</b>
1.1	The outgrowth in numbers of inorganic–organic hybrid materials reported in Cambridge Structural Database during 1990 to 2011.	2
1.2	Proposed classification of hybrid materials, according to the dimensionality of the ultimate structures with respect to the organic connectivity between metal centers ( $O^n$ ) and extended inorganic connectivity ( $I^n$ ).	4
1.3	Illustration of design strategies in inorganic crystal engineering by means of different building blocks and dimensional increasing fashions.	5
1.4	Numbers of the first–row transition metals–organic hybrid frameworks deposited in Cambridge Structure Database, during 1957 – May, 2012.	8
1.5	Numbers of Co-polyamine hybrid frameworks deposited in Cambridge Structure Database, during 1957 – May, 2012.	9
1.6	Diagrams showing different coordination modes reported to the Cambridge Structure Database for the sulfate anions with corresponding Harris notations. Figures in parentheses are numbers of the deposited structures for any metals and lanthanides.	10

1.7	Numbers of the lanthanide metals–organic hybrid frameworks deposited in Cambridge Structure Database, during 1957 – May, 2012.	12
2.1	An ORTEP view of the extended asymmetric unit of <b>I</b> drawn at 80% probability level with hydrogen atoms omitted for clarity. Symmetry codes: (i) $[-x, -y + 2, -z]$ (ii) $[x, y + 1, z]$ (iii) $[-x + 0.5, y + 0.5, -z + 0.5]$ (iv) $[-x + 1, -y + 1, -z]$ .	24
2.2	A polyhedral view of the $(\{UuDd\}:T.)\beta$ -POV layer in <b>I</b> .	27
2.3	View of the 3–D structure of <b>I</b> with hydrogen bonds shown in dotted lines.	28
2.4	Powder X–ray diffraction pattern of compound <b>I</b> (a) simulated (b) experimental XRD patterns.	30
2.5	FT–IR spectrum collected on the ground crystals of compound <b>I</b> .	31
3.1	Crystal appearances of compound (A) <b>III</b> and (B) <b>IV</b> .	37
3.2	ORTEP representation of the asymmetric unit of <b>III</b> drawn at 50% thermal ellipsoids with hydrogen atoms omitted for clarity.	42
3.3	Illustration of the 1–D coordination polymer chain $([Co(4,4'\text{-bipy})(H_2O)_4]^{2+})$ within <b>III</b> .	44

- 3.4 (A) Hydrogen bonding of sulfate S(1) linking two  $\text{Co}(\text{H}_2\text{O})_4$  units. 46  
Symmetry codes: (ii)  $[-x + 0.5, y - 0.5, -z + 0.5]$  (iii)  $[x + 0.5, -y + 0.5, z + 0.5]$  (iv)  $[-x + 1, -y, -z + 1]$  (B) Augmented  $R_4^2(8)$  embrace between two  $\text{Co}(\text{H}_2\text{O})_4$  units mediated by sulfate S(2). Symmetry code: (v)  $[-x + 1, -y + 1, -z + 1]$ .
- 3.5 Representation of the hydrogen-bonded chain in **III** composed entirely 48  
of sulfate and unbound water which runs parallel to  $[101]$ . Symmetry codes: (ix)  $[x - 0.5, -y + 1.5, z - 0.5]$  (x)  $[x + 1, y, z + 1]$ .
- 3.6 (A) Space filling representation of the bipyridinium cation 50  
( $\text{C}_{10}\text{N}_2\text{H}_{10}$ )<sup>2+</sup> occluded within the coordination polymer and hydrogen bonding framework. (B) ORTEP representation of the bipyridinium cation and the interactions it makes to the surrounding species. Short contacts which are indicative of favorable interactions are shown as dashed lines.
- 3.7 ORTEP representation of the asymmetric unit of **IV**. Atoms are drawn 52  
as 50% thermal ellipsoids. Carbon and hydrogen atoms have not been labeled to aid clarity. Similarly only the major orientation of the disordered sulfate is labeled.
- 3.8 Part of the infinite coordination polymer chain in **IV** representing one 57  
period of the sinusoidal chain.
- 3.9 N–Co–N angle in transition metal–4,4'–bipy compounds (from 595 57  
examples with angles greater than  $155^\circ$ ).

3.10	The structure of <b>IV</b> viewed down [100] showing the interdigitated $\text{Co}^{\text{II}}$ -4,4'-bipy chains and six-membered rings of the 3-D hydrogen bonding network.	59
3.11	3D hydrogen bonded array in <b>IV</b> created from $\text{Co}^{\text{II}}$ , sulfate and water.	60
3.12	Thermogravimetric analysis (TGA) of compound <b>III</b> .	62
3.13	Thermogravimetric analysis (TGA) of compound <b>IV</b> .	63
3.14	FT-IR spectra of compound (a) <b>III</b> and (b) <b>IV</b> .	66
3.15	FT- Raman spectra of compound (a) <b>III</b> and (b) <b>IV</b> .	66
3.16	UV-visible spectra of compound (a) <b>III</b> and (b) <b>IV</b> .	67
4.1	Le Bail fit of the compound <b>VIa</b> .	73
4.2	Powder X-ray diffraction pattern of compound <b>V</b> .	75
4.3	Powder X-ray diffraction patterns of compound <b>VIa</b> and <b>VIb</b> .	75
4.4	Powder X-ray diffraction patterns of compound <b>VIIa</b> , <b>VIIb</b> and <b>VIIc</b> .	76
4.5	Room temperature IR spectra of the compounds.	76
4.6	ORTEP diagram of extended asymmetric unit of compound <b>V</b> .	80
	Thermal ellipsoids are given at 80% probability. Symmetry codes: (i) $[x + 1, y, z]$ (ii) $[x - 1, y, z]$ (iii) $[-x + 1, -y + 1, -z + 2]$ (iv) $[-x, -y + 1, -z + 2]$ (v) $[-x, -y, -z + 2]$ (vi) $[-x, -y, -z + 1]$ .	
4.7	The distorted tricapped trigonal prismatic geometry of the central metal ion of compound <b>V</b> .	81

- 4.8 View of the 2-D infinite La–O–La layer in **V**. Only the lanthanide ion connectivity is shown. 81
- 4.9 View of the 2-D lanthanide sulfate layer in the *ab* plane in **V**. 83
- 4.10 The arrangement of layers in the *bc* plane (**V**). Note that the 4,4'–bipy molecules occupy interlamellar spaces along with the water molecules. 83
- 4.11 ORTEP diagram of extended asymmetric unit of compound **VIb**. 85  
Thermal ellipsoids are given at 80% probability. Symmetry codes: (i)  $[-x+1, -y, -z]$  (ii)  $[x, y+1, z]$  (iii)  $[x+1, y, z]$  (iv)  $[-x+1, -y+2, -z+1]$ .
- 4.12 The distorted tricapped trigonal prismatic geometry of the central metal ion of compound **VIb**. 85
- 4.13 The 1-D infinite Pr–O–Pr chains observed in  $[C_{10}H_{10}N_2]_{0.5} [Pr(SO_4)_2(H_2O)_2]$ , **VIb**. 88
- 4.14 View of the 2-D praseodymium sulfate layer in the *ab* plane. Note that the bound water molecules project out of the plane of the layers.  $S(1)O_4$  and  $S(2)O_4$  are represented by light grey and dark grey polyhedral, respectively. 88
- 4.15 1-D edge-shared ladder-like chain, running along *b* axis in compound **VIb**. 89
- 4.16 3-D arrangement of the layers in the *bc* plane. 89

- 4.17 ORTEP diagram of extended asymmetric unit of compound **VIIa**. 91  
 Thermal ellipsoids are given at 80% probability. Symmetry codes: (i)  $[x, y + 1, z]$  (ii)  $[-x + 1, -y, -z + 1]$  (iii)  $[-x + 1, -y + 1, -z + 1]$  (iv)  $[x, y - 1, z]$  (v)  $[-x, -y, -z + 1]$ .
- 4.18 The distorted tricapped trigonal prismatic and distorted square antiprismatic geometry of the central metal ions of compound **VIIa**. 91
- 4.19 View of the tetrameric unit found in  $[\text{C}_{10}\text{H}_{10}\text{N}_2][\text{Nd}_2(\text{SO}_4)_4(\text{H}_2\text{O})_2]_2$ , **VIIa**. 94
- 4.20 The 2-D layer in the *ab* plane. 95
- 4.21 3-D arrangement of the layers in **VIIa**. 95
- 4.22 The lanthanide ion connectivity in the structures: (A) the honeycomb layer in **V**; (B) the square-grid layer in **VIb**; (C) the honeycomb layer in **VIIa**. 97
- 4.23 Thermogravimetric analysis (TGA) of compound **V**. 99
- 4.24 Thermogravimetric analysis (TGA) of compounds **VIa** and **VIb**. 99
- 4.25 Thermogravimetric analysis (TGA) of compounds **VIIa**, **VIIb** and **VIIb**. 100
- 4.26 Room temperature photoluminescence spectra of compound **V** and the corresponding  $\text{Eu}^{\text{III}}$  and  $\text{Tb}^{\text{III}}$  doped samples. (A) (a) Compound **V**, (b) 4 mol% and (c) 8 mol%  $\text{Eu}^{\text{III}}$  doped samples. (B) (a) Compound **V**, (b) 4 mol% and (c) 8 mol%  $\text{Tb}^{\text{III}}$  doped samples. 102

- 4.27 Room temperature photoluminescence spectra of compound **VIa** and the corresponding  $\text{Eu}^{\text{III}}$  and  $\text{Tb}^{\text{III}}$  doped samples. (A) (a) Compound **VIa**, (b) 4 mol% and (c) 8 mol%  $\text{Eu}^{\text{III}}$  doped samples. (B) (a) Compound **VIa**, (b) 4 mol% and (c) 8 mol%  $\text{Tb}^{\text{III}}$  doped samples. 103
- 4.28 Room temperature luminescence decay of the  ${}^5D_0 \rightarrow {}^7F_1$  emission band for the 4 mol%  $\text{Eu}^{\text{III}}$  doped compound (A) **V** and (B) **VIa**. 104
- 4.29 Room temperature luminescence decay of the  ${}^5D_4 \rightarrow {}^7F_6$  emission band for the 4 mol%  $\text{Eu}^{\text{III}}$  doped compound (A) **V** and (B) **VIa**. 105
- 4.30 Room temperature UV–Vis spectra of compound **VIIa**. 106
- 4.31 The schematic energy level diagram for  $\text{Nd}^{\text{III}}$  in compound **VIIa**. 107
- 4.32 Room temperature upconversion spectra of compound **VIIa**, using 582 nm radiation. 108
- 4.33 The observed emission dependence on the excitation intensity of  $[\text{Nd}_2(\text{SO}_4)_4(\text{H}_2\text{O})_2](\text{C}_{10}\text{H}_{10}\text{N}_2)$ , **VIIa**. (a) 100%, (b) 90.32% (c) 85.19%, (d) 81.34%, (e) 74.86%, (f) 69.38% and (g) 63.56%. 109
- 4.34 The log–log plot of the excitation intensity dependence of the luminescence intensity for  $\lambda = 373, 432, \text{ and } 445 \text{ nm}$ . 110
- 5.1 Ortep view of coordination environments of La ions in **VIII**, with displacement ellipsoids (70% probability) and atomic labeling for non–hydrogen atoms. Symmetry codes: (i)  $[-x + 1, -y + 2, -z + 1]$  (ii)  $[x - 1, y, z]$  (iii)  $[-x, -y + 2, -z + 1]$ . 119

- 5.2 Schematic depictions of the pseudo-tricapped trigonal prismatic units 121  
of two non-equivalent lanthanum ions. Symmetry codes: (i)  $[-x + 1, -y + 2, -z + 1]$  (ii)  $[x - 1, y, z]$  (iii)  $[-x, -y + 2, -z + 1]$ .
- 5.3 (A) Relative orientation of the edge-shared pseudo-tricapped trigonal 122  
prismatic dimers, and (B) the chelating *o-phen* ligands. Symmetry  
codes: (i)  $[-x + 1, -y + 2, -z + 1]$  (iii)  $-x, -y + 2, -z + 1]$ .
- 5.4 Illustrations of coordination mode adopted by three distinct sulfate 123  
anions. Symmetry codes: (i)  $[-x + 1, -y + 2, -z + 1]$  (iii)  $[-x, -y + 2, -z + 1]$  (vi)  $[x + 1, y, z]$ .
- 5.5 Views of (A) the intra- and (B) the inter-chain hydrogen bonding 125  
interactions (dotted lines). Symmetry codes: (iv)  $[-x + 1, -y + 2, -z]$   
(vii)  $[-x + 2, -y + 1, -z]$  (viii)  $[x + 1, y, z - 1]$  (ix)  $[x + 2, y - 1, z - 1]$ .
- 5.6 Views of hydrogen bonding patterns: (A)  $R_2^2(8)$ , (B)  $R_2^2(14)$ , (C) 127  
 $R_2^2(18)$  and (D)  $R_2^2(24)$ . Symmetry codes: (iv)  $[-x + 1, -y + 2, -z]$  (vii)  
 $[-x + 2, -y + 1, -z]$  (viii)  $[x + 1, y, z - 1]$  (ix)  $[x + 2, y - 1, z - 1]$ .
- 5.7 Supramolecular assembly of the 1-D  $[\text{La}_2(\text{o-phen})_2(\text{SO}_4)_3(\text{H}_2\text{O})_2]_n$  128  
chains in solid state *via* hydrogen bonding interactions (dotted lines).
- 5.8 Statistics on molecular curvature of the chelating *o-phen* reported in 128  
the Cambridge Structure Database.
- 5.9 IR spectra of (a) the pristine  $[\text{La}_2(\text{o-phen})_2(\text{SO}_4)_3(\text{H}_2\text{O})_2]_n$ , compared 129  
with (b) the brown sample yielded after the heat treatment at 600°C.

- 5.10 UV–Vis spectra of (a) the ground crystals of  $[\text{La}_2(o\text{-phen})_2(\text{SO}_4)_3(\text{H}_2\text{O})_2]_n$  suspended in water, (b) an aqueous solution of the *o*-phen ligand, and (c) the brown sample yielded after the heat treatment at  $600^\circ\text{C}$ . 131
- 5.11 Thermogravimetric curve collected on the ground crystals of the title compound under a flow of  $\text{N}_2$  gas. 132
- 5.12 (a) Powder XRD pattern simulated from single crystal data set of **VIII**, compared with those of (b) the ground crystals of **VIII** (c) the 8 mol%  $\text{Eu}^{\text{III}}$  doped **VIII** (d) the 8 mol%  $\text{Tb}^{\text{III}}$  doped **VIII**, and (e) the brown sample yielded after the heat treatment at  $600^\circ\text{C}$ . 133
- 5.13 Room temperature photoluminescence spectra of (a) the pristine **VIII**, compared with the (b) 4 mol% and (c) 8 mol%  $\text{Eu}^{\text{III}}$  doped samples. 135
- 5.14 Room temperature photoluminescence spectra of (a) the pristine **VIII**, compared with the (b) 4 mol% and (c) 8 mol%  $\text{Tb}^{\text{III}}$  doped samples. 135
- 6.1 Diagrams showing different coordination modes of the carboxylate anions reported to the Cambridge Structure Database. 140
- 6.2 *In situ* synthesis of 2,5-dioxo-piperazine-1,4-diacetic acid (*L2*) from the decomposition reaction of the  $\text{H}_6\text{TTHA}$  ligand under the employed hydrothermal condition. 153

- 6.3 ORTEP view of coordination environments of Pr<sup>III</sup> ions in **IXa** with displacement ellipsoids (60% probability) and atomic labeling for non-hydrogen atoms. Hydrogen atoms are omitted for clarity. 155  
Symmetry codes: (i)  $[-x + 1, -y, -z + 1]$  (ii)  $[-x + 1, -y + 1, -z + 1]$  (iii)  $[-x + 1, -y + 1, -z + 2]$ .
- 6.4 View of (A) pseudo-monocapped square anti-prism of Pr(1) and (B) Pr(2), and (C) bicapped square anti-prism of Pr(2). Symmetry codes: 156  
(i)  $[-x + 1, -y, -z + 1]$  (ii)  $[-x + 1, -y + 1, -z + 1]$  (iii)  $[-x + 1, -y + 1, -z + 2]$ .
- 6.5 The assembly of four Pr(1) and three Pr(2) about the TTHA ligand in **IXa**. Symmetry codes: (ii)  $[-x + 1, -y + 1, -z + 1]$  (iii)  $[-x + 1, -y + 1, -z + 2]$  (iv)  $[x - 1, y, z]$  (v)  $[x, y - 1, z]$ . 157
- 6.6 The structural building dimers in **IXa**;  $\{\text{Pr}(1)_2\text{O}_{16}\}$ ,  $\{\text{Pr}(2)_2\text{O}_{16}\}$  and  $\{\text{Pr}(2)_2\text{O}_{18}\}$ . Symmetry codes: (i)  $[-x + 1, -y, -z + 1]$  (ii)  $[-x + 1, -y + 1, -z + 1]$  (vi)  $[x, y, z - 1]$ . 159
- 6.7 The infinite 1-D chains of regularly alternative  $\{\text{Pr}(1)_2\text{O}_{16}\}$  and  $\{\text{Pr}(2)_2\text{O}_{16}\}$  or  $\{\text{Pr}(2)_2\text{O}_{18}\}$  dimers extending along the  $[0 -\frac{1}{2} \frac{1}{2}]$  direction, which are linked by the  $\mu_7-\eta^{16}$  TTHA ligands. Water of crystallization and hydrogen atoms are omitted for clarity. 160
- 6.8 Infinite 1-D chains made up of the  $\{\text{Pr}(2)_2\text{O}_{18}\}$  dimers and the diprotonated *L2* ligands extending along the  $[-\frac{1}{2} \frac{1}{2} 0]$  direction. 160  
Symmetry codes: (iii)  $[-x + 1, -y + 1, -z + 2]$  (vii)  $[x + 1, y - 1, z]$ .

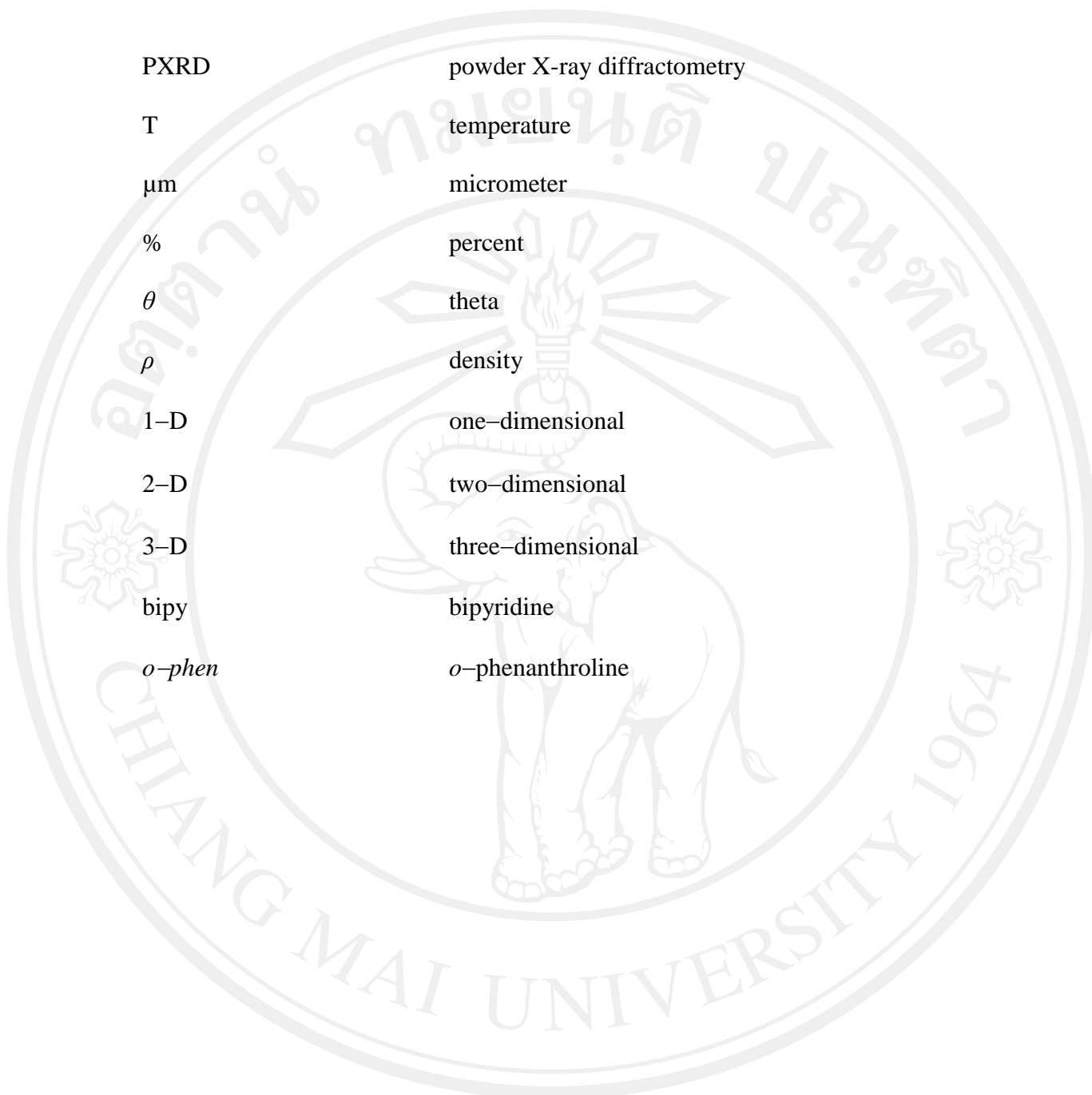
- 6.9 FT-IR spectrum of compound **IXa** with selected band indexing. 161
- 6.10 Dense 3-D framework structure of **IXa**. Water of crystallization and hydrogen atoms are omitted for clarity. 162
- 6.11 ORTEP view of the asymmetric unit of **X** with displacement ellipsoids (60% probability) and atomic labeling for non-hydrogen atoms. Hydrogen atoms are omitted for clarity. Symmetry code: (i)  $[-x + 1, -y + 2, -z]$ . 163
- 6.12 Pseudo-monocapped square anti-prismatic geometry of (A) Sm(1), (B) Sm(2), (C) Sm(3), (D) and (E) Sm(4). Symmetry code: (i)  $[-x + 1, -y + 2, -z]$ . 165
- 6.13 View of coordination modes and relation conformation of carboxylate units in TTHA ligands found in structure **X**. Symmetry codes: (i)  $[-x + 1, -y + 2, -z]$  (ii)  $[-x + 1, -y + 1, -z + 1]$  (iii)  $[-x + 1, y + 1, z]$  (iv)  $[x - 1, y, z]$  (v)  $[-x + 1, -y + 1, -z]$  (vi)  $[-x + 2, -y + 1, -z]$ . 167
- 6.14 The  $\{Sm_8O_{58}\}$  octamer units in **X**. Symmetry code: (iv)  $[x - 1, y, z]$ . 168
- 6.15 The 1-D  $\{Sm_8O_{58}\}$  octamers lying in the  $[\frac{1}{2} -1 \frac{1}{2}]$  direction. Water of crystallization and hydrogen atoms are omitted for clarity. Symmetry code: (iv)  $[x - 1, y, z]$ . 169
- 6.16 Dense 3-D framework of **X**. Water of crystallization and hydrogen atoms are omitted for clarity. 169

- 6.17 The 1-D chain of *L2* ligand and two adjacent Sm(4) ions in *a* direction. Symmetry codes: (iv)  $[x - 1, y, z]$  (vii)  $[-x + 1, -y, -z + 1]$  (viii)  $[-x + 2, -y, -z + 1]$ . 170
- 6.18 FT-IR spectrum of compound **X** with selected band indexing. 170
- 6.19 ORTEP presentation of the asymmetric unit of **XIa** with displacement ellipsoids (60% probability) and atomic labeling for non-hydrogen atoms. Hydrogen atoms are omitted for clarity. Symmetry codes: (i)  $[-x, -y, -z + 2]$  (ii)  $[-x, -y, -z + 1]$  (iii)  $[-x, -y + 1, -z + 1]$  (iv)  $[x - 1, y, z]$  (v)  $[-x, -y + 1, -z + 2]$  (vi)  $[x - 1, y + 1, z]$ . 172
- 6.20 View of the Pr<sup>III</sup> and the surrounding TTHA ligands. (A) Pr(1) (B) Pr(2) with O(17) and (C) Pr(2) with O(14) and O(16) as a ligand. Symmetry codes: (i)  $[-x, -y, -z + 2]$  (iii)  $[-x, -y + 1, -z + 1]$ . 174
- 6.21 The disorder of the sulfate anion. Symmetry codes: (ii)  $[-x, -y, -z + 1]$ . 175
- 6.22 The structural building dimers;  $\{\text{Pr}(1)_2\text{O}_{16}\}$  and  $\{\text{Pr}(2)_2\text{O}_{16}\}$ . Symmetry codes: (i)  $[-x, -y, -z + 2]$  (ii)  $[-x, -y, -z + 1]$  (iii)  $[-x, -y + 1, -z + 1]$ . 176
- 6.23 The condensation of 1-D chains viewed along  $[0 -\frac{1}{2} \frac{1}{2}]$  axis. 176
- 6.24 The 3.1110 bridging mode of the sulfate anion linking the  $\{\text{Pr}(1)\text{O}_9\}$  and  $\{\text{Pr}(2)\text{O}_9\}$  motifs of 1-D chain along  $[0 -\frac{1}{2} \frac{1}{2}]$  and the  $\{\text{Pr}(2)\text{O}_9\}$  with the adjacent  $\{\text{Pr}(2)\text{O}_9\}$  along the *b* direction. Symmetry codes: (ii)  $[-x, -y, -z + 1]$ . 177

- 6.25 The assembly of five Pr(1) and three Pr(2) about the TTHA ligand in **XIa**. Symmetry codes: (iii)  $[-x, -y + 1, -z + 1]$  (iv)  $[x - 1, y, z]$  (v)  $[-x, -y + 1, -z + 2]$  (vi)  $[x - 1, y + 1, z]$  (vii)  $[x, y + 1, z]$ . 178
- 6.26 Circular channels extending along  $b$  axis in **XIa**. 178
- 6.27 View of the extended asymmetric unit of **XII** and the pseudo-monocapped square anti-prismatic geometry of  $\text{Sm}(1)^{\text{III}}$  with displacement ellipsoids (70% probability) and atomic labeling for non-hydrogen atoms. Hydrogen atoms are omitted for clarity. Symmetry codes: (i)  $[-x + 0.5, -y + 0.5, -z]$  (ii)  $[-x + 1, y, -z + 0.5]$ . 181
- 6.28 View of the  $\{\text{Sm}^{\text{III}}_2\text{O}_{18}\}$  dimer and the surrounding TTHA ligands. Symmetry codes: (i)  $[-x + 0.5, -y + 0.5, -z]$ . 181
- 6.29 Arrangement of  $\{\text{Sm}^{\text{III}}_2\text{O}_{18}\}$  dimer viewed along  $a$  direction. 182
- 6.30 The assembly of six Sm(1) about the TTHA ligand in **XII**. Symmetry codes: (ii)  $[-x + 1, y, -z + 0.5]$  (iii)  $[-x + 1, -y, -z]$  (iv)  $[-x + 0.5, y + 0.5, -z + 0.5]$  (v)  $[x + 0.5, y - 0.5, z]$  (vi)  $[x, -y, z + 0.5]$ . 182
- 6.31 (A) Elliptical channels lying along  $[1\ 1\ 0]$  direction and (B) Circular channels lying along  $c$  direction. 184

## ABBREVIATIONS AND SYMBOLS

Å	angstrom
<i>ca.</i>	<i>circa</i> (approximately)
cm <sup>3</sup>	cubic centimeter
°C	degree Celsius
<i>etc.</i>	<i>et cetara</i>
<i>et al.</i>	<i>et alibi</i>
EDS	energy dispersive X-ray spectroscopy
<i>e.g.</i>	<i>exempli gratia</i> (for example)
SEM	scanning electron microscopy
g	gram
h	hours
<i>i.e.</i>	<i>id est</i> (that is)
K	Kelvin
K/s	Kelvin per second
kHz	kilohertz
mA	milliampere
min	minute
mm	millimeter
MHz	megahertz
nm	nanometer



PXRD	powder X-ray diffractometry
T	temperature
$\mu\text{m}$	micrometer
%	percent
$\theta$	theta
$\rho$	density
1-D	one-dimensional
2-D	two-dimensional
3-D	three-dimensional
bipy	bipyridine
<i>o</i> -phen	<i>o</i> -phenanthroline